

1 **GIS-Based DRASTIC and Composite DRASTIC Indexes for Assessment Groundwater**
2 **Vulnerability in Baghin Aquifer, Kerman, Iran**

3 Mohammad Malakootian¹, Majid Nozari^{2,*}

4 **Manuscript Authors details:**

5 1. Mohammad Malakootian, Department of Environmental Health, School of Public Health,
6 Kerman University of Medical Sciences, Iran. E-mail: m.malakootian@yahoo.com.
7 <https://orcid.org/0000-0002-4051-6242>.

8 2. Majid Nozari, Department of Environmental Health, School of Public Health, Kerman
9 University of Medical Sciences, Iran. Tel: 98-9383921819, E-mail: nozari.m@kmu.ac.ir.
10 <https://orcid.org/0000-0003-2319-1930>.

11 **ABSTRACT**

12 The present study estimated the Kerman–Baghin aquifer vulnerability using DRASTIC and
13 composite DRASTIC (CDRASTIC) indexes. Factors affecting the transfer of contamination,
14 including water table depth, soil media, aquifer media, impact of vadose zone, topography,
15 hydraulic conductivity, and land use, were ranked, weighted, and integrated, using a
16 geographical information system (GIS). A sensitivity test was also performed to determine
17 parameters sensitivity. Results showed that the topographic layer displays a gentle slope in the
18 aquifer. Most of the aquifer was covered with irrigated field crops and grassland with a moderate
19 vegetation cover. In addition, the aquifer vulnerability maps indicated very similar results,
20 recognizing the northwest parts of the aquifer as areas with high to very high vulnerability. The
21 map removal sensibility analysis (MRSA) reveal that the impact of vadose zone (in the
22 DRASTIC index) and hydraulic conductivity (in the CDRASTIC index) as the most important

23 parameters in the vulnerability evaluation. In both indexes, the single-parameter sensibility
24 analysis (SPSA) showed net recharge as the most effective factor in the vulnerability estimation.
25 From this study, it could be concluded that vulnerability maps could be used as a tool to control
26 human activities for protection and sustainable usage.

27 **Keywords:** Vulnerability; Sensitivity Analyses; DRASTIC; Composite DRASTIC; Kerman–
28 Baghin Aquifer

29 1. Introduction

30 Groundwater is a significant and principal freshwater resource in most parts of the world,
31 especially for arid and semi-arid areas. Water quality has been emphasized more in groundwater
32 management (Neshat et al., 2014; Manap et al., 2013; Manap et al., 2014a; Ayazi et al., 2010).
33 The potential groundwater contamination by human activities at or near the surface of
34 groundwater has been considered the major base to manage this resource by implementing
35 preventative policies (Tilahun and Merkel, 2010).

36 Groundwater vulnerability is a measure of how easy or how hard it is for pollution or
37 contamination at the land surface to reach a production aquifer. In other words, it is a measure of
38 the “degree of insulation” that natural and manmade factors provide to keep pollution away from
39 groundwater (Sarah and Patricia, 1993; Neshat et al., 2014). Vulnerability maps are commonly
40 performed at the sub-region and regional scales. Normally, they are not applied to site-specific
41 evaluations, including zones smaller than a few tens of square kilometers (Baalousha, 2006;
42 Tilahun and Merkel, 2010). Various techniques have been developed to assess groundwater
43 susceptibility with great precision (Javadi et al., 2010; Javadi et al., 2011). Most of the methods
44 are based on analytic tools to associate groundwater contamination to land operations. There are

45 three types of evaluation methods: the process-based simulations, the statistic procedures and,
46 and the overlay and index approaches (Neshat et al., 2014; Dixon, 2004).

47 Process-based approach involves numerical modeling and is useful at the local but not the
48 regional level. Statistical approach involves correlating actual water quality data to spatial
49 variables and requires a large amount of site specific data (National Research Council, 1993).

50 Overlay and index procedures affirm the incorporation of various zonal maps by allocating a
51 numeral index. Both procedures are simple to use in the geographic information system,
52 especially on a zonal measure. Hence, these methods are the most popular procedures applied to
53 vulnerability estimation (Neshat et al., 2014). The overlay and index methods have some

54 significant advantages; firstly, they have become popular because the methodology is fairly
55 straightforward that can be easily implemented with any GIS application software. The concept
56 of overlaying data layers is easily comprehended even by less experienced users. In addition, the
57 data requirement could be considered as moderate, since nowadays most data come in digital
58 format. Hydrogeological information is either available or could be estimated using relevant
59 data. Consequently, these methods give relatively accurate results for extensive areas with a
60 complex geological structure. Lastly, the product of this approach could be easily interpreted by
61 water-resource managers and could be incorporated into decision-making processes. Even a
62 simple visual inspection of the vulnerability map can reveal important contamination hotspots.
63 Probably the most important and obvious disadvantage of these methods raised by scientists and
64 experts is the inherent subjectivity in the determination of the rating scales and the weighting
65 coefficients (National Research Council, 1993).

66

67

68 The most extensively used methods for the groundwater vulnerability evaluation are GODS
69 (Ghazavi and Ebrahimi, 2015), IRISH (Daly and Drew, 1999), AVI (Raju et al., 2014), and
70 DRASTIC (Neshat et al., 2014; Baghapour et al., 2014; Baghapour et al., 2016).

71 The DRASTIC index, proposed by Aller et al (1985), is considered as one of the best
72 indexes for groundwater vulnerability estimation. This method ignores the influence of zonal
73 properties. Thus, identical weights and rating values are utilized. In addition, this technique fails
74 to apply a standard validation test for the aquifer. Therefore, several investigators developed this
75 index using various techniques (Neshat et al., 2014). The higher DRASTIC index represents the
76 greater contamination potential and inversely. After calculating the DRASTIC index, it should be
77 possible to identify the zones that are more prone to pollution. This index only provides a
78 relative estimation and is not created to make a complete assessment (Baalousha, 2006).

79 Many studies have been conducted using DRASTIC index to estimate the groundwater
80 vulnerability in different regions of the world (Jaseela et al., 2016; Zghibi et al., 2016; Kardan
81 Moghaddam et al., 2017; Kumar et al., 2016; Neshat and Pradhan, 2017; Souleymane and Tang,
82 2017; Ghosh and Kanchan, 2016; Saida et al., 2017); however, there are still a number of studies
83 that used the CDRASTIC index for groundwater vulnerability evaluation (Baghapour et al.,
84 2016; Baghapour et al., 2014; Secunda et al., 1998; Jayasekera et al., 2011; Shirazi et al., 2012;
85 Jayasekera et al., 2008). Boughriba et al. (2010) utilized DRASTIC index in geographical
86 information system environment to estimate the aquifer vulnerability. They provided the
87 DRASTIC modified map prepared from total DRASTIC indexes and small monitoring network
88 maps including high and medium classes. Then, authors integrated the map with land use map to
89 provide the contamination potential map. They reported the new obtained groundwater
90 vulnerability map, including three various classes, namely very high, high, and medium. Babiker

91 et al. (2005) used the DRASTIC index to determine point's prone to contamination from human
92 activities in the aquifer. They reported that the western and eastern parts of the aquifer fall in the
93 high and medium classes, respectively in terms of vulnerability. The final aquifer vulnerability
94 map represented that the high risk of pollution is in the eastern part of aquifer due to agriculture
95 activities. They also observed that net recharge inflicts the largest impact on the aquifer
96 vulnerability, followed by soil media, topography, the impact of vadose zone, and hydraulic
97 conductivity.

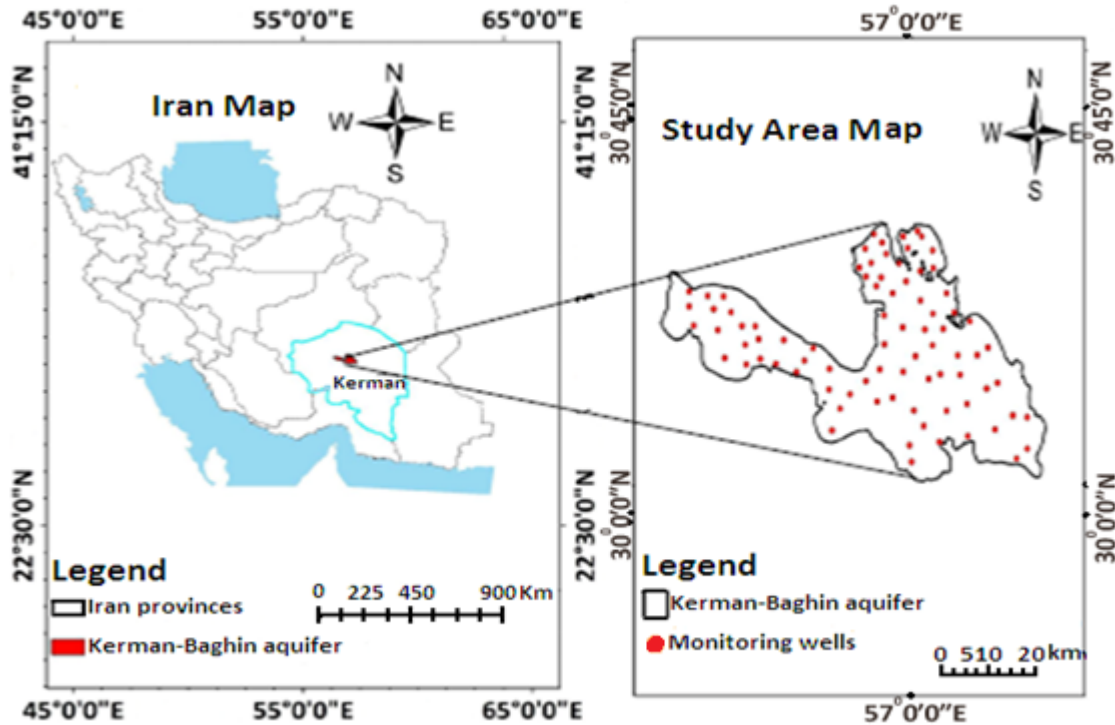
98 The average annual precipitation in Iran is 257 mm (namely less than one-third of the average
99 annual precipitation at the global level). Water scarcity is a very critical and serious problem in
100 Iran (Chitsazan and Akhtari, 2006; Modabberi et al., 2017). In addition, the groundwater
101 reduction makes the problem even worse. Groundwater is the only freshwater resource in the
102 Kerman province, due to the lack of surface water. The Baghin aquifer is located in the central
103 part of Kerman province of Iran. Due to recent droughts, this aquifer has been under heavy
104 pumping stress to irrigate crops, which caused a graduated drop of water level. Consequently,
105 this could increase contamination potential in the aquifer. Therefore, the aim of this research was
106 to provide a vulnerability map for the Kerman–Baghin aquifer and performing a sensitivity
107 analysis to identify the most influential factors in vulnerability assessment.

108 2. Methods and Materials

109 2.1. Study Area

110 Kerman Province covers both arid and semi-arid lands. The present study included a 2023 km²
111 area (29° 47' to 30° 31' N latitude and 56° 18' to 57° 37' E longitude) located in the central part of
112 Kerman Province, Iran (Figure 1). The study area is mostly covered with agricultural lands
113 (Neshat et al., 2014). The mean annual rainfall is 108.3 mm (during 2017) in the study area; the

114 highest and lowest topographic elevation is 1,980 and 1,633 m above sea level; and eventually,
 115 the mean, minimum, and maximum annual temperatures are 17°C, -12°C, and 41°C, respectively
 116 (during 2017).



117
 118 **Figure 1.** Location map of the Kerman–Baghin aquifer

119 **2.2. DRASTIC and CDRASTIC Indexes Computation**

120 DRASTIC is a procedure developed by the United States Environmental Protection Agency (U.S
 121 EPA) to evaluate the groundwater pollution (Aller et al., 1985). The DRASTIC index is obtained
 122 using the following relation (Kardan Moghaddam et al., 2017; Neshat and Pradhan, 2017):

123
$$\text{DRASTIC index} = D_r D_w + R_r R_w + A_r A_w + S_r S_w + T_r T_w + I_r I_w + C_r C_w \quad (1)$$

124 **where** DRASTIC comprises the effective factors in the DRASTIC index. D, R, A, S, T, I, and C
 125 stand for water table depth, net recharge, aquifer media, soil media, topography, impact of
 126 vadose zone, and hydraulic conductivity, respectively. In addition, “r” and “w” are the rating and

127 weight of each factor, respectively. The ratings and weights of factors are presented in Table 1.
 128 A high DRASTIC index corresponds to a high vulnerability of the aquifer to pollution. In the
 129 DRASTIC index, each parameter is rated on a scale from 1 to 10 that shows the relative
 130 contamination potential of that parameter for that area. In addition, in the DRASTIC index, one
 131 weight (1 to 5) is assigned to each of the parameters. Weight values show the relative
 132 significance of the parameters with respect to each other. Ranges of vulnerability corresponding
 133 to the DRASTIC index are presented in Table 2.

134 **Table 1** Rating and weight related to DRASTIC index factors (Aller et al., 1985)

DRASTIC parameters	Range	Rating (r)	Weight (w)
Water table depth (m)	0.0-1.5	10	
	1.5-4.6	9	
	4.6-9.1	7	
	9.1-15.2	5	5
	15.2-22.9	3	
	22.9-30.5	2	
	>30.5	1	
Net recharge	11-13	10	
	9-11	8	
	7-9	5	4
	5-7	3	
	3-5	1	
Aquifer media	Rubble and sand	9	
	Gravel and sand	7	
	Gravel, sand, clay, and silt	5	3
	Sand and clay	4	
	Sand, clay, and silt	3	
Soil media	Rubble, sand, clay, and silt	9	
	Gravel and sand	7	
	Gravel, sand, clay, and silt	6	
	Sand	5	2
	Sand, clay, and silt clay and silt	3 2	
Topography or slope (%)	0-2	10	
	2-6	9	
	6-12	5	1
	12-18	3	
	>18	1	

The impact of the vadose zone	Rubble, sand, clay, and silt	9	5
	Gravel and sand	7	
	Gravel, sand, clay, and silt	5	
	Sand, clay, and silt	3	
Hydraulic conductivity (m/day)	0-4.1	1	3
	4.1-12.2	2	
	12.2-28.5	4	
	28.5-40.7	6	
	40.7-81.5	8	

135 **Table 2** Range of vulnerability related to the DRASTIC index

Vulnerability	Ranges
Very low	23-46
Low	47-92
Moderate	93-136
High	137-184
Very high	>185

136 To obtain the CDRASTIC index, an additional factor (land use) is added to the above relation.

137 Thus, the CDRASTIC index was obtained as follows:

138
$$\text{CDRASTIC index} = D_r D_w + R_r R_w + A_r A_w + S_r S_w + T_r T_w + I_r I_w + C_r C_w + L_r L_w \quad (2)$$

139 where L_w and L_r are the relative weight and rating related to land use, respectively. Ratings and
140 weightings applied to the pollution potential are shown in Table 3 which are related to land use
141 based on the CDRASTIC index. The final outputs of CDRASTIC relation range from 28 to
142 280. Vulnerability ranges based on the CDRASTIC index are presented in Table 4.

143 **Table 3** Ratings and weighting applied to pollution potential related to land use based on
144 CDRASTIC index (Aller et al., 1985)

Land use	Rating	Weight
Irrigated field crops + Urban areas	10	
Irrigated field crops + Grassland with poor vegetation cover + Urban areas	9	
Irrigated field crops + Grassland with moderate vegetation cover + Urban areas	8	
Irrigated field crops	8	
Irrigated field crops + Fallow land + Grassland with poor vegetation cover	7	
Irrigated field crops + Grassland with poor vegetation cover	7	
Irrigated field crops + Grassland with moderate vegetation cover	6	

Irrigated field crops + Rocky + Urban areas	5	5
Irrigated field crops + Grassland with poor vegetation cover + Woodland	5	
Irrigated field crops + Woodland	5	
Irrigated field crops + Rocky	4	
Fallow land	3	
Fallow land + Grassland with poor vegetation cover	3	
Fallow land + Grassland with moderate vegetation cover	3	
Grassland with poor vegetation cover	2	
Grassland with moderate vegetation cover	2	
Grassland with moderate vegetation cover + Woodland	1	
Sand dune + Grassland with moderate vegetation cover	1	
Sand dune	1	

145 **Table 4** Vulnerability ranges related to CDRASTIC index

Vulnerability	Ranges
Very low	<100
Low	100-145
Moderate	145-190
High	190-235
Very high	≥235

146 **2.3. Factors Affecting Transfer of Contamination**

147 Water table depth is the distance of water table from ground surface in a well (Baghapour et al.,
148 2016). Eighty-three wells were utilized in the Kerman–Baghin aquifer to obtain this factor. The
149 interpolation procedure was used to provide a raster map of the water table depth, which was
150 categorized based on Table 2.

151 Net recharge is the amount of runoff that penetrated into the ground and reaches the
152 groundwater surface (Singh et al., 2015; Ghosh and Kanchan, 2016). This research used the
153 Piscopo method (Chitsazan and Akhtari, 2009) to provide net recharge layer for the Kerman–
154 Baghin aquifer according to the following equation and Table 5:

155 Net recharge slope (%) + rainfall + soil permeability. (3)

156 In the above equation, the percentage of slope was calculated from a topographical map, using
157 a digital elevation model. In addition, a soil permeability map was created using the Kerman–

158 Baghin aquifer soil map (with scale 1:250000) and the drilling logs of 83 wells. In the end, a map
 159 of rainfall rate in the area was compiled based on annual average precipitation. Ratings and
 160 weights of net recharge are presented in Table 5.

161 **Table 5** Weight, rating, and range of net recharge (Aller et al., 1985)

Slope (%)		Rainfall		Soil permeability		Net Recharge		
Range (%)	Factor	Range (mm/year)	Factor	Range	Factor	Range (cm/year)	Rating	Weight
<2	4	>850	4	High	5	11-13	10	
2-10	3	700-850	3	Moderate to high	4	9-11	8	
10-33	2	500-700	2	Moderate	3	7-9	5	4
>33	1	<500	1	Low	2	5-7	3	
				Very low	1	3-5	1	

162 Aquifer media controls the movement of groundwater streams in the aquifer (Aller et al.,
 163 1985; Singh et al., 2015). To obtain this layer, drilling log data of 83 wells were used. Data were
 164 collected from Kerman Regional Water Office (KRWO). The range of the aquifer media layer is
 165 shown in Table 2.

166 Soil media has a considerable impact on the amount of water surface that can penetrate into
 167 the aquifer. Therefore, where the soil layer is thick, the debilitation processes such as absorption,
 168 filtration, degradation, and evaporation may be considerable (Singh et al., 2015). A soil media
 169 raster map was provided using the Kerman–Baghin aquifer soil map and the wells drilling logs.
 170 The range of the soil media layer is presented in Table 2.

171 Topography controls the residence time of water inside on the soil and the degree of
 172 penetration (Singh et al., 2015). To obtain this layer, the percentage of the slope was provided
 173 from the topographical map, using a digital elevation model. Data were collected from the
 174 KRWO. The range of the topographic layer is presented in Table 2.

175 Vadose zone is the unsaturated area located between the topographic surface and the
 176 groundwater level (Singh et al., 2015). It plays a significant role in decreasing groundwater

177 contamination by pollutant debilitation processes such as purification, chemical reaction, and
178 dispersal (Shirazi et al., 2012). This study used the lithologic data of 83 observation and
179 exploration wells to design the impact of vadose zone raster map of aquifer. Data were collected
180 from the KRWO. The range of the impact of vadose zone layer is depicted in Table 2.

181 Hydraulic conductivity refers to the capability of the aquifer to transfer water. High hydraulic
182 conductivity areas demonstrate a high potential for groundwater contamination (Singh et al.,
183 2015; Aller et al., 1985). To prepare this layer, data derived from pumping tests of wells were
184 used. The range of hydraulic conductivity layer is shown in Table 2.

185 Land use influences groundwater resources via variation in recharge amount and by changing
186 freshwater demands for water. Land use is obligatory since it is required by the CDRASTIC
187 index. The Indian remote sensing satellite information was utilized to provide land use raster
188 map. The weight and rating related to land use layer are presented in Table 3.

189 **2.4. Sensitivity Analyses**

190 One of the main advantages of the DRASTIC index is the evaluation performance because, a
191 high number of input data are used, and this allows to restrict the effects of errors on final results.
192 Nevertheless, some authors, namely Babikeret al. (2005), Barber et al.(1993), and Merchant
193 (1994), reported that similar results could be obtained using fewer data and at lower costs. The
194 unavoidable subjectivity related to the choosing seven factors, ranks, and weights used to
195 calculate the vulnerability index has also been criticized. Therefore, in order to eliminate the
196 aforementioned criticisms, two sensitivity analyses were performed as follows (Napolitano and
197 Fabbri, 1996):

198 **A. Map Removal Sensibility Analysis (MRSA)**

199 MRSA value indicates the vulnerability map sensibility to removal of one or more maps from the
200 suitability analysis. MRSA is calculated as follows (Babiker et al., 2005; Martínez-Bastida et al.,
201 2010; Saidi et al., 2011; Modabberi et al., 2017):

$$202 \quad S = \left[\left| \frac{\frac{V}{N} - \frac{V'}{n}}{V} \right| \right] \times 100, \quad (4)$$

203 where S stands for the sensibility value expressed in terms of variation index, V is the intrinsic
204 vulnerability index (real vulnerability index) and V' is the intrinsic vulnerability index after
205 removing X; N and n are the number of data used to calculate V and V', respectively (Babiker et
206 al., 2005; Martínez-Bastida et al., 2010; Saidi et al., 2011; Modabberi et al., 2017).

207 **B. Single-Parameter Sensibility Analysis (SPSA)**

208 SPSA was first introduced by Napolitano and Fabbri (1996). This test shows the effect of each
209 DRASTIC factor on the final vulnerability index. Using this test derived from Equation 5, the
210 real and effective weight of each factor, compared to the theoretical weight assigned by the
211 analytical model was calculated by Babiker et al(2005), Martínez-Bastida et al (2010), Saidi et
212 al(2011) and Modabberi et al (2017);

$$213 \quad W = \left[\frac{P_r P_w}{V} \right] \times 100, \quad (5)$$

214 where W is the effective weight of each factor. P_r and P_w are the rank and weight assigned to P,
215 respectively. V is the intrinsic vulnerability index (Martínez-Bastida et al., 2010; Babiker et al.,
216 2005; Saidi et al., 2011; Modabberi et al., 2017).

217 **3. Results and Discussion**

218 **3.1. DRASTIC and CDRASTIC Parameters**

219 Based on data shown in Table 2, the assigned rating of water table depth varies from 1 to 10. In
220 addition, based on the results presented in Table 6, water table depth in the aquifer varies from

221 4.6 to >30.5 m (rating 1 to 7). About 27.55% of the aquifer has a depth greater than 30.5 m, and
222 66.16 % of the aquifer has a depth ranging from 9.1 m and 30.5 m. Less than 7% of the aquifer
223 has a depth between 4.6 m and 9.1 m. The Kerman–Baghin aquifer rated map of water table
224 depth is presented in Figure 2(A). According to Figure 2(A) and Table 6, the minimum impact of
225 water table depth on aquifer vulnerability occurs in the central parts (6.39%), whereas the
226 maximum impact occurs in the north, south, northwest, and southeast parts (27.55%).

227 According to the results presented in Table 6, 75.81% of the aquifer has a net recharge value
228 from 7 to 9 cm/year. A net recharge value between 9 and 11 cm/year was found for 11.74% of the
229 aquifer. The Kerman–Baghin aquifer rated map of net recharge is shown in Figure 2(B).
230 According to Piscopo's method, the Kerman–Baghin aquifer was divided into three classes, with
231 regard to net recharge. The highest net recharge value was observed in the north, northeast,
232 south, southwest, parts of the northwest, parts of the center, and parts of the southeast (75.81%),
233 whereas the least net recharge value appeared in parts of the northwest and center (11.74%), as
234 shown in Figure 2(B) and Table 6.

235 As observed in Table 6, the majority of the Kerman–Baghin aquifer media is composed of
236 sand, clay, and silt (75.21%). The Kerman–Baghin aquifer rated map of aquifer media is
237 presented in Figure 3(A). Parts of the aquifer in the north, northwest, northeast, center, and
238 southeast are composed of sand, clay, and silt. Parts of the aquifer in the northwest are composed
239 of rubble and sand (5.58%). Parts of the aquifer in the south and northwest are composed of
240 gravel and sand (8.95%), and gravel, sand, clay, and silt (10.26%).

241 The Kerman–Baghin aquifer rated map of soil media is presented in Figure 3(B). The soil
242 map depicts six different soil classes. The highest rank (rank = 9) was assigned to rubble, sand,
243 clay, and silt (a combination of rubble, sand, clay and silt soils). In addition, the lowest rank

244 (rank = 2) was assigned to clay and silt(a combination of clay and silt soils). Most of the aquifer
245 soil media is covered with silt, sand, and clay (about 80%).

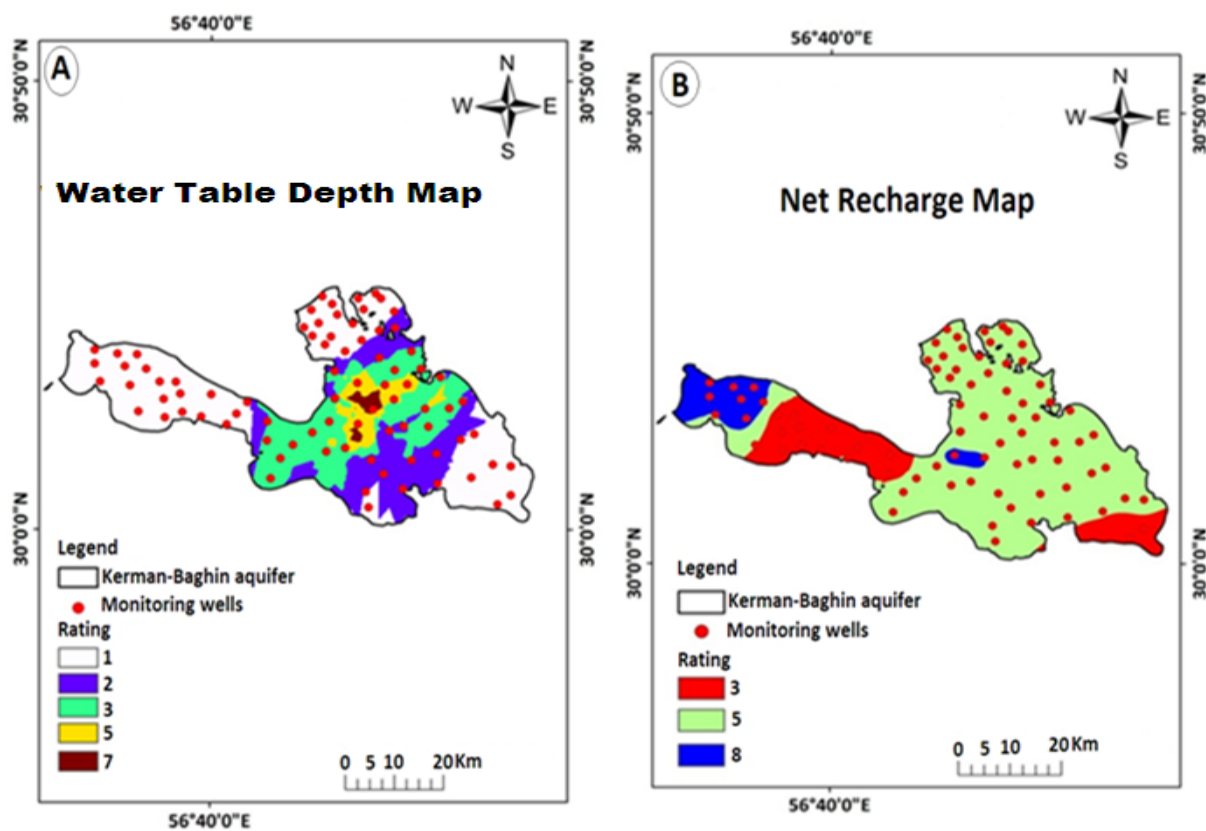
246 The Kerman–Baghin aquifer rated map of topography is shown in Figure 4(A). The
247 topographical layer shows a gentle slope (0 to 6%) over most of the aquifer, hence gaining ranks
248 of 9 and 10. A slope range of 0 to 2% includes 34.72% of the study area, and its rating (slope
249 range = 0–2%) is 10. In addition, 65.28% of the aquifer has a slope range of 2 to 6% (parts of the
250 northwest) as shown in Figure 4(A) and Table 6. As the gradient increases, the runoff increases
251 as well (Israil et al., 2006) leading to less penetration (Jaiswal et al., 2003). According to
252 Madrucci et al. (2008), the gradients higher than 35° are considered restrictions on groundwater
253 desirability because of the lack of springs.

254 The Kerman–Baghin aquifer rated map of the impact of vadose zone is indicated in Figure
255 4(B). According to the results, the soil with a rank of 5 (gravel, sand, clay, and silt) is more
256 effective in aquifer vulnerability (35.47%). Other various types of soils such as sand, clay, and
257 silt (parts of the north, northeast, south, and southeast), gravel and sand (parts of the center and
258 northwest), and rubble, sand, clay, and silt (parts of the northwest) cover 34.24%, 20.39%, and
259 9.9% of the aquifer, respectively, as shown in Figure 4(B) and Table 6. Sandy soil is effective on
260 groundwater occurrence because of the high rate of penetration (Srivastava and Bhattacharya,
261 2006). However, clay soil is arranged poorly because of low infiltration (Manap et al., 2014b).

262 The Kerman–Baghin aquifer rated map of hydraulic conductivity is presented in Figure 5(A).
263 Hydraulic conductivity shows high variability. Our study results show that hydraulic
264 conductivity of the Kerman–Baghin aquifer varied from 0 to 81.5 m/day. The potential for
265 groundwater contamination was greater in zones with high hydraulic conductivity (38.27%). As
266 shown in Figure 5(A) and Table 6, 29.51%, 23.93%, 5.98%, and 2.31% of the study areas have

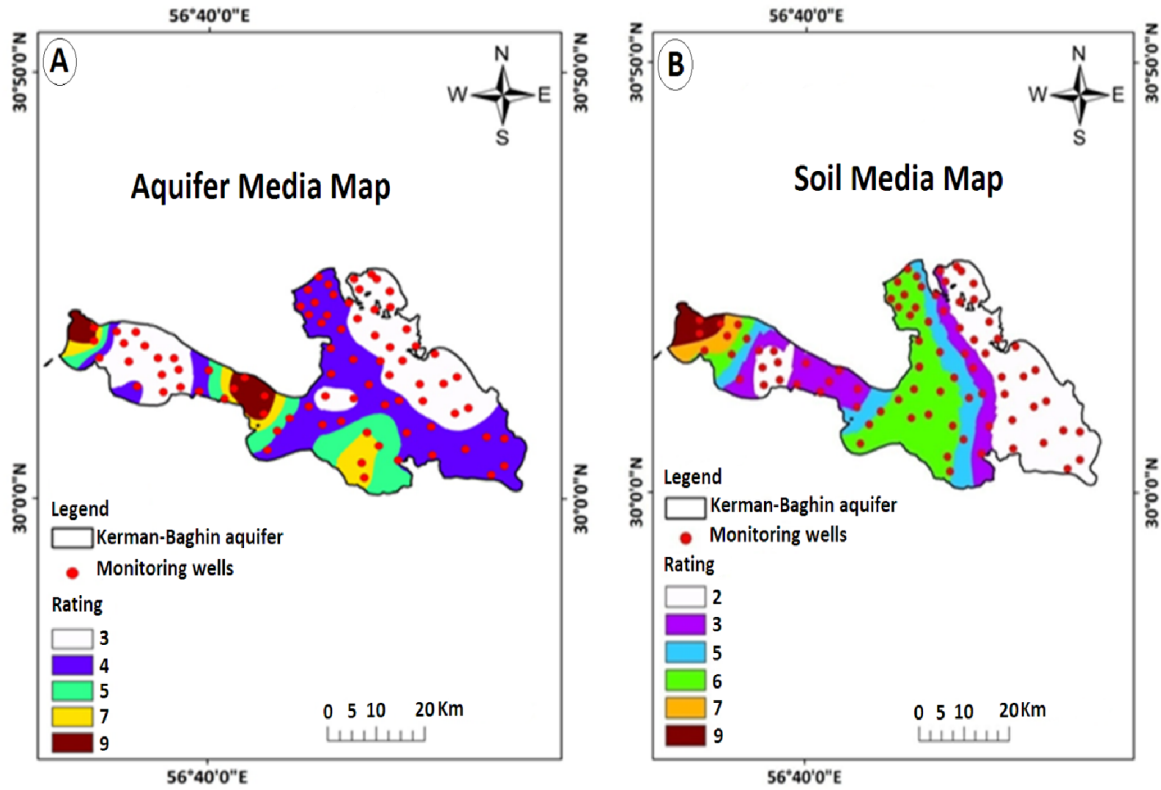
267 hydraulic conductivity in the ranges of 0 to 4.1 m/day, 12.2 to 28.5 m/day, 28.5 to 40.7 m/day,
268 and 40.7 to 81.5 m/day, respectively.

269 The Kerman–Baghin aquifer rated map of land use is presented in Figure 5(B). Our results
270 show that the majority of the Kerman–Baghin aquifer is covered with irrigated field crops and
271 grassland with moderate vegetation cover (20.45%). Less than 4% of the study area is irrigated
272 field crops and urban areas (3.61%), and 58.47% of the study area is irrigated field crops with
273 urban areas, grassland with poor and moderate vegetation cover, fallow land, woodland, and
274 rocky ground. In addition, 10.17% of the study area is fallow land with poor grassland and
275 moderate vegetation, and 13.72% of the study area is sand dunes with poor grassland and
276 moderate vegetation cover and woodland as shown in Figure 5(B) and Tables 3 and 6.



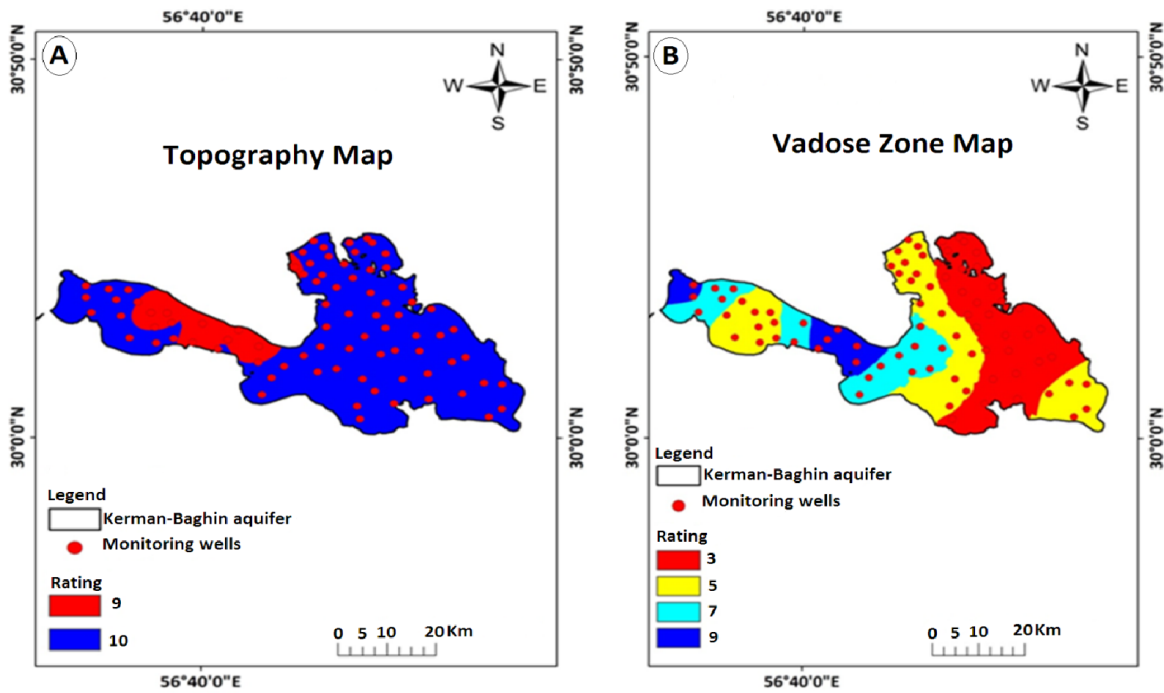
277

278 **Figure 2.** Kerman–Baghin aquifer rated maps of A) water table depth and B) net recharge



279
280

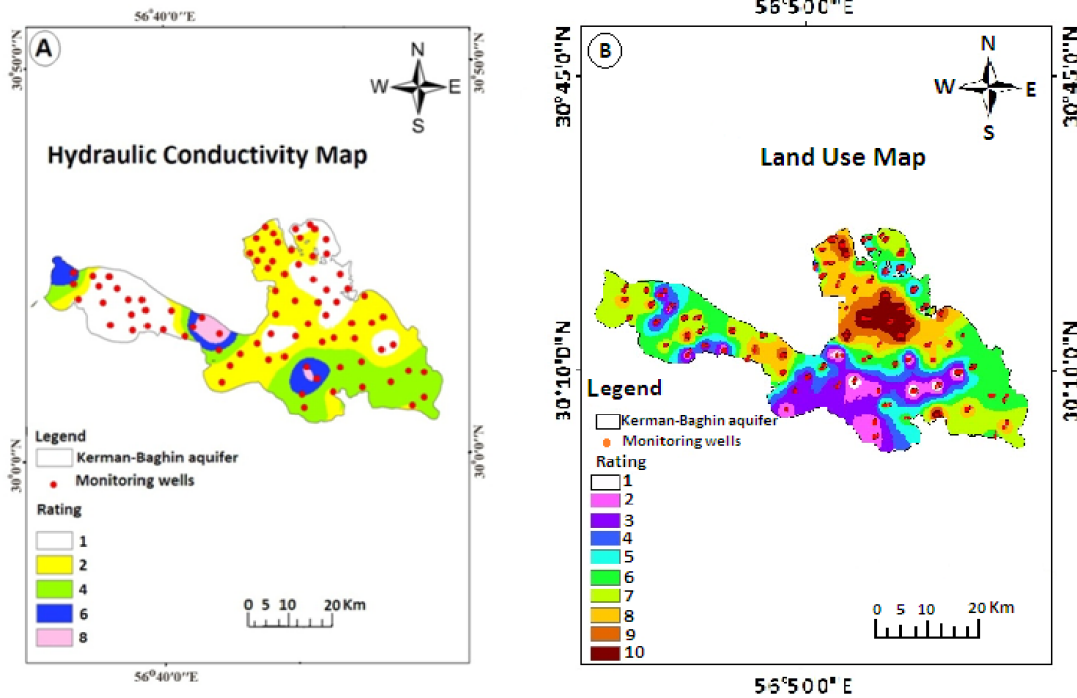
Figure 3. Kerman–Baghin aquifer rated maps of A) aquifer media and B) soil media



281

282

Figure 4. Kerman–Baghin aquifer rated maps of A) topography and B) vadose zone



283

284 **Figure. 5.** Kerman–Baghin aquifer rated maps of A) hydraulic conductivity and B) land use

285 **Table 6** Area of rating (km² and %) of DRASTIC and CDRASTIC parameters

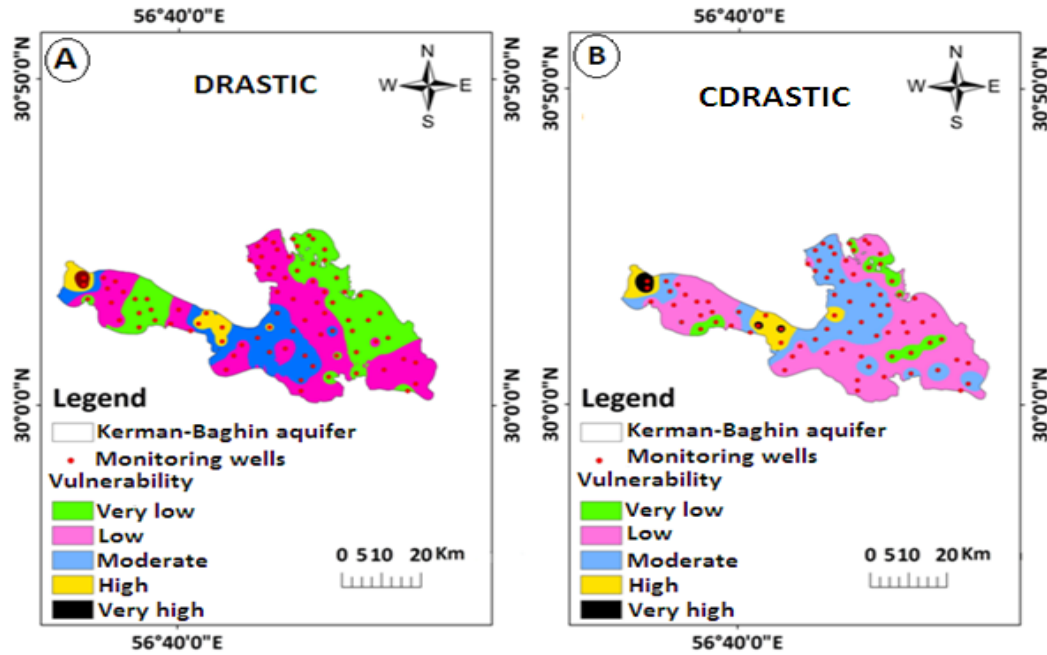
DRASTIC and CDRASTIC indexes parameters	Rating	Area (km ²)	Area (%)	The aquifer geographic directions covered by the respective rating in the parameters rated maps
Water table depth	1	557.73	27.55	Parts of the north, south, northwest, and southeast
	2	472.18	23.34	Parts of the north, south, and center
	3	469.78	23.29	Parts of the center
	5	395.00	19.53	Parts of the center
	7	129.14	6.39	Parts of the center
Net recharge	3	252.04	12.45	Parts of southeast, and northwest
	5	1534.15	75.81	North, northeast, south, southwest, and parts of the northwest, center, southeast
	8	237.6	11.74	Parts of the northwest and center
Aquifer media	3	743.18	36.72	Parts of the north, northwest, northeast, and center
	4	779.01	38.49	Parts of the north, northwest, southeast, and center
	5	207.81	10.26	Parts of the south, and northwest
	7	181.02	8.95	Parts of the south, and northwest
	9	112.76	5.58	Parts of the northwest
Soil media	2	658.5	32.53	Parts of the north, northwest, northeast, and southeast
	3	399.72	19.75	Parts of the north, northwest, south, and center

	5	297.44	14.69	Parts of the north, northwest, south, and center
	6	538.77	26.62	Parts of the northwest, center, and southwest
	7	67.56	3.33	Parts of the northwest
	9	61.79	3.08	Parts of the northwest
Topography	9	702.74	34.72	North, northwest, northeast, south, southeast, southwest, and center
	10	1321.07	65.28	parts of the northwest
The impact of the vadose zone	3	692.87	34.24	Parts of the north, northeast, south, and southeast
	5	717.91	35.47	Parts of the north, northwest, south, southeast, and center
	7	412.49	20.39	Parts of the center, and northwest
	9	200.53	9.9	Parts of the northwest
Hydraulic conductivity	1	597.11	29.51	Parts of the northeast, northwest, southeast, and center
	2	774.52	38.27	parts of the northwest, south, southeast, and center
	4	484.17	23.93	Parts of the northwest, south, and southeast
	6	120.99	5.98	Parts of the south, and northwest
	8	46.7	2.31	Parts of the south, and northwest
Land use	1	112.48	5.56	Parts of the south
	2	165.02	8.16	Parts of the south
	3	205.65	10.17	Parts of the south, and center
	4	357.06	17.64	Parts of the south, southwest, northwest, and center
	5	234.86	11.61	Parts of the southeast, northwest, and center
	6	413.86	20.45	Parts of the southeast, northwest, northeast, and center
	7	182.63	9.02	Parts of the north, northwest, and northeast
	8	169.4	8.37	Parts of the north, northwest, and northeast
	9	109.42	5.41	Parts of the north, northwest, and northeast
	10	73.09	3.61	Parts of the north

286 **3.2. DRASTIC and CDRASTIC Vulnerability Indexes**

287 The Kerman–Baghin aquifer vulnerability map obtained using DRASTIC and CDRASTIC
288 indexes is shown in Figure 6. In the studied aquifer, the vulnerability falls under very high, high,
289 moderate, low, and very low vulnerable areas. It is found that in both indexes, the north,
290 northeast, northwest, south, southwest, southeast and center parts come under low and very low
291 vulnerability. This could be attributed to low water depth, hydraulic conductivity, and net

292 recharge characterizing these aquifer areas; another reason might be that the aquifer media is
293 mostly clay, sand and silt soils. The vulnerability area, identified by investigated indexes, is
294 illustrated in Table 7. Low and very low vulnerable zones cover 25.21% and 38.31% of the
295 Kerman–Baghin aquifer respectively using DRASTIC index. Very low and low vulnerable zones
296 cover 24.95% and 40.41%, respectively, using the CDRASTIC index. This is primarily due to
297 water table depth and relatively low permeability of vadose zone in such aquifers (Colins et al.,
298 2016). About 26% of the studied aquifer had moderate groundwater pollution potential, using
299 DRASTIC and CDRASTIC indexes. This does not mean that such areas are without pollution;
300 rather, they are relatively prone to pollution when compared to other areas (Colins et al., 2016).
301 From the DRASTIC index values, it was found that 10.4% of the study aquifer was under high
302 (8.46%) and very high (1.94%) vulnerability. The results of the study showed that 8.75% of the
303 aquifer is in the ranges of 190 to 235 and greater than 235 in the CDRASTIC index (Table 7).
304 According to these two indexes, the vulnerability maps indicated very same findings, showing
305 the northwest portion of the aquifer as high and very high vulnerable zones. The high
306 vulnerability can be attributed to great water depth, hydraulic conductivity, and net recharge in
307 these aquifer areas. In addition, this can be due to the great slope in this area.



308

309 **Figure 6.** Vulnerability maps of Kerman–Baghin aquifer by DRASTIC and CDRASTIC indexes

310 **Table 7** Area of vulnerability (km² and %) identified by DRASTIC and CDRASTIC indexes

Vulnerability	DRASTIC				CDRASTIC			
	Ranges	Area (km ²)	Area (%)	The aquifer geographic directions covered by the respective vulnerability	Ranges	Area (km ²)	Area (%)	The aquifer geographic directions covered by the respective vulnerability
Very low	23-46	510.25	25.21	Parts of the south, north, northwest, and northeast	<100	505.02	24.95	Parts of the southeast, north, northwest, and northeast
Low	47-92	775.14	38.31	Parts of the south, southwest, southeast, north, northwest, northeast, and center	100-145	817.70	40.41	Parts of the south, southwest, southeast, north, northwest, northeast, and center
Moderate	93-136	527.85	26.08	Parts of the south, southwest, northwest, and center	145-190	524.06	25.89	Parts of the south, southwest, southwest, northwest, and center
High	137-184	171.02	8.46	Parts of the northwest	190-235	126.91	6.28	Parts of the northwest and center
Very high	>185	39.23	1.94	Parts of the northwest	≥235	49.79	2.47	Parts of the northwest

311

312 3.3. Sensitivity of DRASTIC Model

313 The MRSA, the DRASTIC index, is performed by eliminating one layer data at a time as

314 indicated in Table 8. The results showed a high variation in vulnerability index when the impact

315 of vadose zone was removed, so that, the average variation index was 1.88%. This shows that the
316 factor is more effective in vulnerability assessment using the DRASTIC index. When this
317 parameter is removed from the overlay process, this leads to a significant decrease in
318 vulnerability index. This could be due to the high theoretical weight assigned to this factor
319 (weight = 5). These findings are similar to those obtained by Dibi et al. (2012) who have shown
320 that, in addition to this parameter, topography, net recharge, and water table depth have a high
321 impact on the vulnerability index. In addition, in Samake et al. (2011), the impact of vadose zone
322 and hydraulic conductivity had a significant impact on vulnerability index, that appears to have a
323 moderate sensitivity to deletion of water table depth (1.48%), net recharge (1.36%), and
324 hydraulic conductivity (1.25%). The minimum menu variation index was achieved after
325 eliminating the aquifer media (0.44%), as indicated in Table 8.

326 To estimate the effect of individual factors on aquifer vulnerability, the SPSA was performed.
327 A summary of results of SPSA in the DRASTIC index are shown in Table 9. The SPSA
328 compares the effective and theoretical weights. The average effective weight of net recharge was
329 43.26% and its theoretical weight (%) was 17.4%. This shows that the factor is more effective in
330 vulnerability assessment using the DRASTIC index. The results reported by other studies
331 (Babiker et al., 2005; Doumouya et al., 2012) are similar to those of the present study. The
332 impact of vadose zone and water table depth had high theoretical weights (21.74%); they have
333 been dedicated with an effective weight with average value such as 8.33% and 25.55%. The
334 remaining factors showed an average effective weights of 14.91% (aquifer media), 9.89% (soil
335 media), 11.35% (topography), and 7.01% (hydraulic conductivity). The theoretical weights
336 assigned to water table depth, net recharge, topography, and hydraulic conductivity were not in

337 agreement with the effective weight. The highest and lowest impact on aquifer vulnerability was
 338 related to net recharge and hydraulic conductivity, respectively (Table 9).

339 **Table 8** Statistical results of MRSA in the DRASTIC index

The sensitivity of variability index (S) (%)				Removed parameters
SD	Min.	Max.	Ave.	
0.414	0.05	2.36	1.36	D
0.775	0.07	3.06	1.48	R
0.311	0.05	1.31	0.44	A
0.486	0.00	1.65	0.73	S
0.339	0.03	1.31	0.51	T
0.894	0.25	3.84	1.88	I
0.550	0.03	1.98	1.25	C

340 **Table 9** Statistical results of SPSA in the DRASTIC index

Effective weight (%)				Theoretical weight (%)	Theoretical Weight	Parameters
SD	Min.	Max.	Ave.			
6.179	3.23	28.46	8.33	21.74	5	D
11.998	14.06	73.47	43.26	17.4	4	R
3.190	7.26	22.13	14.91	13.04	3	A
2.916	4.49	14.29	9.89	8.7	2	S
2.222	6.45	14.71	11.35	4.3	1	T
5.367	15.79	37.31	25.55	21.74	5	I
3.738	2.42	18.75	7.01	13.04	3	C

341 **3.4. Sensibility of CDRASTIC index**

342 The MRSA in the CDRASTIC index was performed by eliminating one data layer at a time as
 343 indicated in Table 10. The mean variation index of hydraulic conductivity was 4.13%. Hydraulic
 344 conductivity had a greater effect on the aquifer vulnerability followed by water table depth
 345 (4.05%), soil media (3.82%), topography (3.68%), aquifer media (3.28%), net recharge (2.72%),
 346 the impact of vadose zone (2.33%), and land use (1.99%).

347 The effective weight derived from the SPSA to the CDRASTIC index is shown in Table 11.
 348 The average effective weight of net recharge was 32.62%. This shows that the factor is more
 349 effective in vulnerability assessment using CDRASTIC index. Hydraulic conductivity displays
 350 the lowest effective weights (5.32%). Topography, net recharge, and land use had upper effective
 351 weights toward the theoretical weights specified by CDRASTIC index. The average effective

weight of land use was 24.82%. This shows that the parameter was the second effective parameter in aquifer vulnerability, using the CDRASTIC index (Table 11).

Table 10 Statistical results of MRSA in CDRASTIC index

The sensitivity of variability index (S) (%)				Removed parameters
SD	Min.	Max.	Ave.	
1.403	0.50	6.48	4.05	D
1.617	0.11	10.91	2.72	R
1.541	0.06	5.99	3.28	A
1.508	0.67	6.60	3.82	S
1.353	0.87	5.87	3.68	T
1.439	0.06	5.12	2.33	I
1.480	0.55	6.72	4.13	C
0.375	1.23	3.00	1.99	L

Table 11 Statistical results of SPSA in CDRASTIC index

Effective weight (%)				Theoretical weight (%)	Theoretical Weight	Parameters
SD	Min.	Max.	Ave.			
4.849	2.63	26.88	6.27	21.74	5	D
10.672	10.4	66.67	32.62	17.4	4	R
3.026	6.29	20.00	11.23	13.04	3	A
2.621	3.31	12.96	7.5	8.7	2	S
1.609	5.2	12.82	8.45	4.3	1	T
4.648	10.87	32.05	19.2	21.74	5	I
3.134	2.1	14.88	5.32	13.04	3	C
10.122	3.88	42.37	24.82	17.85	5	L

4. Conclusions

Evaluations of vulnerability indexes for the Kerman–Baghin aquifer were conducted using the GIS-based DRASTIC and CDRASTIC indexes. Seven hydro–geological factors (as the letters of the acronym show) were considered in the determination of aquifer vulnerability using DRASTIC, and eight parameters were considered in the CDRASTIC approach. From the DRASTIC index values, it was determined that 10.4% of the aquifer is under high (8.46%) to very high (1.94%) vulnerability. From the CDRASTIC index values, it was determined that 8.75% of the aquifer is under high (6.28%) to very high (2.47%) vulnerability. In addition, we found that parts of the north, south, southeast, and northwest have low to very low vulnerability based on the DRASTIC and CDRASTIC indexes. The MRSA signifies the fact that hydraulic

366 conductivity and the impact of vadose zone induce a high risk of aquifer contamination
367 according to the DRASTIC and CDRASTIC indexes, respectively. For both methods, the SPSA
368 analysis shows that net recharge has a high risk to aquifer contamination. The results of this
369 study showed that parts of the Kerman–Baghin aquifer tend to be contaminate that needs to be
370 considered by regional authorities. Regarding urban planning and the organization of agricultural
371 activities in Kerman Province, the vulnerability map prepared in the study could be the most
372 important when considering protection of groundwater quality. In areas with high and very high
373 vulnerability to groundwater pollution, there should be restrictions on soil fertilization as well as
374 permanent pasture, or afforestation should be introduced in the arable land. In addition, these
375 areas should not be converted into housing developments. In addition, groundwater vulnerability
376 maps of the Kerman–Baghin aquifer are ideal to be used in future land-use planning.

377 **Acknowledgments**

378 The authors would like to thank the Environmental Health Engineering Research Center,
379 Kerman University of Medical Sciences, for their scientific support.

380 **Competing interests.** The authors declare that they have no conflict of interest.

381 **References**

382 Aller, L., Truman, b., Jay H, L., Rebecca J, P., and Glen, H.: DRASTIC: a standardized system
383 for evaluating ground water pollution potential using hydrogeologic settings, U.S Environmental
384 Protection Agency, USA, 1985.

385 Ayazi, M. H., Pirasteh, S., Arvin, A., Pradhan, B., Nikouravan, B., and Mansor, S.: Disasters and
386 risk reduction in groundwater: Zagros Mountain Southwest Iran using geoinformatics
387 techniques, Disaster Adv., 3, 51-57, 2010.

388 Baalousha, H.: Vulnerability assessment for the Gaza Strip, Palestine using DRASTIC, J.
389 Environ. Geol., 50, 405-414, <https://doi.org/10.1007/s00254-006-0219-z>, 2006.

390 Babiker, I. S., Mohamed, M. A., Hiyama, T., and Kato, K.: A GIS-based DRASTIC model for
391 assessing aquifer vulnerability in Kakamigahara Heights, Gifu Prefecture, central Japan, Sci
392 Total Environ., 345, 127-140, <https://doi.org/10.1016/j.scitotenv.2004.11.005>, 2005.

393 Baghapour, M. A., Talebbeydokhti, N., Tabatabaee, H., and Nobandegani, A. F.: Assessment of
394 groundwater nitrate pollution and determination of groundwater protection zones using
395 DRASTIC and composite DRASTIC (CD) models: the case of Shiraz unconfined aquifer, J.
396 Health. Sci. Surveill. Syst., 2, 54-65, 2014.

397 Baghapour, M. A., Nobandegani, A. F., Talebbeydokhti, N., Bagherzadeh, S., Nadiri, A. A.,
398 Gharekhani, M., and Chitsazan, N.: Optimization of DRASTIC method by artificial neural
399 network, nitrate vulnerability index, and composite DRASTIC models to assess groundwater
400 vulnerability for unconfined aquifer of Shiraz Plain, Iran, J Environ Health Sci Eng., 14, 1-16,
401 <https://doi.org/10.1186/s40201-016-0254-y>, 2016.

402 Barber, C., Bates, L. E., Barron, R., and Allison, H.: Assessment of the relative vulnerability of
403 groundwater to pollution: a review and background paper for the conference workshop on
404 vulnerability assessment, AGSO J Aust Geol Geophys., 14, 147-154, 1993.

405 Boughriba, M., Barkaoui, A.-e., Zarhloule, Y., Lahmer, Z., El Houadi, B., and Verdoya, M.:
406 Groundwater vulnerability and risk mapping of the Angad transboundary aquifer using
407 DRASTIC index method in GIS environment, Arab J Geosci., 3, 207-220,
408 <https://doi.org/10.1007/s12517-009-0072-y>, 2010.

409 Chitsazan, M., and Akhtari, Y.: Evaluating the potential of groundwater pollution in Kherran and
410 Zoweircherry plains through GIS-based DRASTIC model, *J. Water. Wastewater*, 17, 39-51,
411 2006.

412 Chitsazan, M., and Akhtari, Y.: A GIS-based DRASTIC model for assessing aquifer
413 vulnerability in Kherran Plain, Khuzestan, Iran, *Water Resour Manag.*, 23, 1137-1155,
414 <https://doi.org/10.1007/s11269-008-9319-8>, 2009.

415 Colins, J., Sashikkumar, M., Anas, P., and Kirubakaran, M.: GIS-based assessment of aquifer
416 vulnerability using DRASTIC Model: A case study on Kodaganar basin, *Earth Sci. Res. J.*, 20, 1-
417 8, <https://doi.org/10.15446/esrj.v20n1.52469>, 2016.

418 Daly, D., and Drew, D.: Irish methodologies for karst aquifer protection, in: Beek B (ed)
419 Hydrogeology and engineering geology of sinkholes and karst, Balkema, Rotterdam, 267-272,
420 1999.

421 Dibi, B., Kouame, K. I., Konan-Waidhet, A. B., Savane, I., Biemi, J., Nedeff, V., and Lazar, G.:
422 Impact of agriculture on the quality of groundwater resources in peri-urban zone of Songon
423 (Cote D'ivoire), *Environ. Engine. Manage. J.*, 11, 2173-2182,
424 <https://doi.org/10.30638/eemj.2012.271>, 2012.

425 Dixon, B.: Prediction of ground water vulnerability using an integrated GIS-based Neuro-Fuzzy
426 techniques, *J. Spat. Hydro.*, 4, 1-38, 2004.

427 Doumouya, I., Dibi, B., Kouame, K. I., Saley, B., Jourda, J. P., Savane, I., and Biemi, J.:
428 Modelling of favourable zones for the establishment of water points by geographical information
429 system (GIS) and multicriteria analysis (MCA) in the Aboisso area (South-east of Côte d'Ivoire),
430 *Environ. Earth. Sci.*, 67, 1763-1780, <https://doi.org/10.1007/s12665-012-1622-2>, 2012.

431 Ghazavi, R., and Ebrahimi, Z.: Assessing groundwater vulnerability to contamination in an arid
432 environment using DRASTIC and GOD models, *Inte. J. Environ. Sci. Tech*, 12, 2909-2918,
433 <https://doi.org/10.1007/s13762-015-0813-2>, 2015.

434 Ghosh, T., and Kanchan, R.: Aquifer vulnerability assessment in the Bengal alluvial tract, India,
435 using GIS based DRASTIC model, *Model Earth Syst Environ.*, 2, 2-13,
436 <https://doi.org/10.1007/s40808-016-0208-5>, 2016.

437 Israil, M., Al-hadithi, M., Singhal, D., Kumar, B., Rao, M. S., and Verma, S.: Groundwater
438 resources evaluation in the Piedmont zone of Himalaya, India, using Isotope and GIS techniques,
439 *J. Spatial. Hydro.*, 6, 107-119, 2006.

440 Jaiswal, R., Mukherjee, S., Krishnamurthy, J., and Saxena, R.: Role of remote sensing and GIS
441 techniques for generation of groundwater prospect zones towards rural development--an
442 approach, *Int J Remote Sens.*, 24, 993-1008, <https://doi.org/10.1080/01431160210144543>, 2003.

443 Jaseela, C., Prabhakar, K., and Harikumar, P. S. P.: Application of GIS and DRASTIC modeling
444 for evaluation of groundwater vulnerability near a solid waste disposal site, *Int. J. Geosci.*, 7,
445 558-571, <https://doi.org/10.4236/ijg.2016.74043>, 2016.

446 Javadi, S., Kavehkar, N., Mousavizadeh, M., and Mohammadi, K.: Modification of DRASTIC
447 model to map groundwater vulnerability to pollution using nitrate measurements in agricultural
448 areas, *J. Agr. Sci. Tech.*, 13, 239-249, 2010.

449 Javadi, S., Kavehkar, N., Mohammadi, K., Khodadadi, A., and Kahawita, R.: Calibrating
450 DRASTIC using field measurements, sensitivity analysis and statistical methods to assess
451 groundwater vulnerability, *Water. Int.*, 36, 719-732,
452 <https://doi.org/10.1080/02508060.2011.610921>, 2011.

453 Jayasekera, D., Kaluarachchi, J. J., and Villholth, K. G.: Groundwater Quality Impacts Due to
454 Population Growth and Land Use Exploitation in the Coastal Aquifers of Sri Lanka, Southern
455 Illinois University Carbondale 2008, 43.

456 Jayasekera, D. L., Kaluarachchi, J. J., and Villholth, K. G.: Groundwater stress and vulnerability
457 in rural coastal aquifers under competing demands: a case study from Sri Lanka, *Environ Monit*
458 *Assess.* , 176, 13-30, <https://doi.org/10.1007/s10661-010-1563-8>, 2011.

459 Kardan Moghaddam, H., Jafari, F., and Javadi, S.: Vulnerability evaluation of a coastal aquifer
460 via GALDIT model and comparison with DRASTIC index using quality parameters, *Hydro. Sci.*
461 *J.*, 62, 137-146, <https://doi.org/10.1080/02626667.2015.1080827>, 2017.

462 Kumar, P., Thakur, P. K., Bansod, B. K., and Debnath, S. K.: Assessment of the effectiveness of
463 DRASTIC in predicting the vulnerability of groundwater to contamination: a case study from
464 Fatehgarh Sahib district in Punjab, India, *Environ. Earth. Sci.*, 75, 879,
465 <https://doi.org/10.1007/s12665-016-5712-4>, 2016.

466 Madrucci, V., Taioli, F., and de Araújo, C. C.: Groundwater favorability map using GIS
467 multicriteria data analysis on crystalline terrain, Sao Paulo State, Brazil, *J. Hydro.*, 357, 153-173,
468 <https://doi.org/10.1016/j.jhydrol.2008.03.026>, 2008.

469 Manap, M. A., Sulaiman, W. N. A., Ramli, M. F., Pradhan, B., and Surip, N.: A knowledge-
470 driven GIS modeling technique for groundwater potential mapping at the Upper Langat Basin,
471 Malaysia, *Arabian. J. Geosci.*, 6, 1621-1637, <https://doi.org/10.1007/s12517-011-0469-2>, 2013.

472 Manap, M. A., Nampak, H., Pradhan, B., Lee, S., Sulaiman, W. N. A., and Ramli, M. F.:
473 Application of probabilistic-based frequency ratio model in groundwater potential mapping using
474 remote sensing data and GIS, *Arabian. J. Geosci.*, 7, 711-724, <https://doi.org/10.1007/s12517-012-0795-z>, 2014a.

476 Manap, M. A., Nampak, H., Pradhan, B., Lee, S., Sulaiman, W. N. A., and Ramli, M. F.:
477 Application of probabilistic-based frequency ratio model in groundwater potential mapping using
478 remote sensing data and GIS, *Arabian. J. Geosci.*, 7, 711-724, [https://doi.org/10.1007/s12517-](https://doi.org/10.1007/s12517-012-0795-z)
479 012-0795-z, 2014b.

480 Martínez-Bastida, J. J., Arauzo, M., and Valladolid, M.: Intrinsic and specific vulnerability of
481 groundwater in central Spain: the risk of nitrate pollution, *Hydro. J.*, 18, 681-698,
482 <https://doi.org/10.1007/s10040-009-0549-5>, 2010.

483 Merchant, J. W.: GIS-based groundwater pollution hazard assessment: a critical review of the
484 DRASTIC model, *Photogramm Eng Remote Sensing.*, 60, 1117-1127, 1994.

485 Modabberi, H., Hashemi, M. M. R., Ashournia, M., and Rahimpour, M. A.: Sensitivity Analysis
486 and Vulnerability Mapping of the Guilan Aquifer Using Drastic Method, *Rev. Environ. Earth.*
487 *Sci.*, 4, 27-41, <https://doi.org/10.18488/journal.80.2017.41.27.41>, 2017.

488 Napolitano, P., and Fabbri, A.: Single-parameter sensitivity analysis for aquifer vulnerability
489 assessment using DRASTIC and SINTACS, *Proceedings of the Vienna Conference,*
490 *Netherlands*, 1996, 559-566.

491 **National Research Council: Ground water vulnerability assessment: Predicting relative**
492 **contamination potential under conditions of uncertainty. National Academies Press, USA, 224,**
493 **1993.**

494 Neshat, A., Pradhan, B., Pirasteh, S., and Shafri, H. Z. M.: Estimating groundwater vulnerability
495 to pollution using a modified DRASTIC model in the Kerman agricultural area, Iran, *Environ.*
496 *Earth. Sci.*, 71, 3119-3131, <https://doi.org/10.1007/s12665-013-2690-7>, 2014.

497 Neshat, A., and Pradhan, B.: Evaluation of groundwater vulnerability to pollution using
498 DRASTIC framework and GIS, *Arabian. J. Geosci.*, 10, 2-8, [https://doi.org/10.1007/s12517-017-](https://doi.org/10.1007/s12517-017-3292-6)
499 3292-6, 2017.

500 Raju, N. J., Ram, P., and Gossel, W.: Evaluation of groundwater vulnerability in the lower
501 Varuna catchment area, Uttar Pradesh, India using AVI concept, *J. Geol. Soc. India.*, 83, 273-
502 278, <https://doi.org/10.1007/s12594-014-0039-9>, 2014.

503 Saida, S., Tarik, H., Abdellah, A., Farid, H., and Hakim, B.: Assessment of groundwater
504 vulnerability to nitrate based on the optimised DRASTIC models in the GIS Environment (Case
505 of Sidi Rached Basin, Algeria), *Geosciences*, 7, 2-23,
506 <https://doi.org/10.3390/geosciences7020020>, 2017.

507 Saidi, S., Bouri, S., and Ben Dhia, H.: Sensitivity analysis in groundwater vulnerability
508 assessment based on GIS in the Mahdia-Ksour Essaf aquifer, Tunisia: a validation study, *Hydro.*
509 *Sci. J.*, 56, 288-304, <https://doi.org/10.1080/02626667.2011.552886>, 2011.

510 Samake, M., Tang, Z., Hlaing, W., Mbue, I. N., Kasereka, K., and Balogun, W. O.: Groundwater
511 vulnerability assessment in shallow aquifer in Linfen Basin, Shanxi Province, China using
512 DRASTIC model, *J. Sustain. Develop.*, 4, 53-71, <https://doi.org/10.5539/jsd.v4n1p53>, 2011.

513 Sarah, C., and Patricia I, C.: Ground water vulnerability assessment: Predicting relative
514 contamination potential under conditions of uncertainty, National Academies Press, USA, 1993.

515 Secunda, S., Collin, M., and Melloul, A. J.: Groundwater vulnerability assessment using a
516 composite model combining DRASTIC with extensive agricultural land use in Israel's Sharon
517 region, *J. Environ. Manage.*, 54, 39-57, <https://doi.org/10.1006/jema.1998.0221>, 1998.

518 Shirazi, S. M., Imran, H., and Akib, S.: GIS-based DRASTIC method for groundwater
519 vulnerability assessment: a review, *J. Risk. Res.*, 15, 991-1011,
520 <https://doi.org/10.1080/13669877.2012.686053>, 2012.

521 Singh, A., Srivastav, S., Kumar, S., and Chakrapani, G. J.: A modified-DRASTIC model
522 (DRASTICA) for assessment of groundwater vulnerability to pollution in an urbanized
523 environment in Lucknow, India, *Environ. Earth. Sci.*, 74, 5475-5490,
524 <https://doi.org/10.1007/s12665-015-4558-5>, 2015.

525 Souleymane, K., and Tang, Z.: A novel method of sensitivity analysis testing by applying the
526 DRASTIC and fuzzy optimization methods to assess groundwater vulnerability to pollution: the
527 case of the Senegal River basin in Mali, *Nat. Hazards. Earth. Sys. Sci.*, 17, 1375-1392,
528 <https://doi.org/10.5194/nhess-17-1375-2017>, 2017.

529 Srivastava, P. K., and Bhattacharya, A. K.: Groundwater assessment through an integrated
530 approach using remote sensing, GIS and resistivity techniques: a case study from a hard rock
531 terrain, *Int. J. Remote. Sens.*, 27, 4599-4620, <https://doi.org/10.1080/01431160600554983>,
532 2006.

533 Tilahun, K., and Merkel, B. J.: Assessment of groundwater vulnerability to pollution in Dire
534 Dawa, Ethiopia using DRASTIC, *Environ. Earth. Sci.*, 59, 1485-1496,
535 <https://doi.org/10.1007/s12665-009-0134-1>, 2010.

536 Zghibi, A., Merzougui, A., Chenini, I., Ergaieg, K., Zouhri, L., and Tarhouni, J.: Groundwater
537 vulnerability analysis of Tunisian coastal aquifer: an application of DRASTIC index method in
538 GIS environment, *Groundwater. Sustain. Develop.*, 2, 169-181,
539 <https://doi.org/10.1016/j.gsd.2016.10.001>, 2016.

540